

# INTEGRAL/IBIS Extragalactic survey: 20-100 keV selected AGN<sup>1</sup>

L. Bassani<sup>2</sup>, M. Molina<sup>3</sup>, A. Malizia<sup>2</sup>, J.B. Stephen<sup>2</sup>, A.J. Bird<sup>3</sup>, A. Bazzano<sup>4</sup>, G. Bélanger<sup>5</sup>, A.J. Dean<sup>3</sup>, A. De Rosa<sup>4</sup>, P. Laurent<sup>5</sup>, F. Lebrun<sup>5</sup>, P. Ubertini<sup>4</sup>, and R. Walter<sup>6</sup>

## ABSTRACT

Analysis of INTEGRAL Core Program and public Open Time observations performed up to April 2005 provides a sample of 62 active galactic nuclei in the 20-100 keV band above a flux limit of  $\sim 1.5 \times 10^{-11} \text{ erg cm}^{-2} \text{ s}^{-1}$ . Most (42) of the sources in the sample are Seyfert galaxies, almost equally divided between type 1 and 2 objects, 6 are blazars and 14 are still unclassified. Excluding the blazars, the average redshift of our sample is 0.021 while the mean luminosity is  $\text{Log}(L) = 43.45$ . We find that absorption is present in 65% of the objects with 14% of the total sample due to Compton thick active galaxies. In agreement with both Swift/BAT team results and 2-10 keV studies, the fraction of absorbed objects decreases with the 20-100 keV luminosity. All Seyfert 2s in our sample are absorbed as are 33% of Seyfert 1s. The present data highlight the capability of INTEGRAL to probe the extragalactic gamma-ray sky and to find new and/or absorbed active galaxies.

*Subject headings:* surveys — galaxies: active — gamma rays: observations

---

<sup>1</sup>Based on observations obtained with the ESA science mission *INTEGRAL*

<sup>2</sup>IASF-Bologna/INAF, via P. Gobetti 101, 40129 Bologna, Italy; bassani@iasfbo.inaf.it, malizia@iasfbo.inaf.it, stephen@iasfbo.inaf.it

<sup>3</sup>School of Physics and Astronomy, University of Southampton, Highfield, Southampton, SO17 1BJ, UK; molinam@astro.soton.ac.uk, ajb@astro.soton.ac.uk, ajd@astro.soton.ac.uk

<sup>4</sup>IASF-Roma/INAF, via del Fosso del Cavaliere 100, I-00133 Roma, Italy; bazzano@rm.iasf.cnr.it, derosa@rm.iasf.cnr.it, ubertini@rm.iasf.cnr.it

<sup>5</sup>CEA Saclay/DSM/DAPNIA/Sap, 91191 Gif Sur Yvette, France; flebrun@cea.fr, fil@discovery.saclay.cea.fr, belanger@hep.saclay.cea.fr

<sup>6</sup>INTEGRAL Science Data Center, Chemin D'Écogia 16, 1290 Versoix, Switzerland; roland.walter@obs.unige.ch

## 1. Introduction

The extragalactic gamma-ray sky is still poorly explored with only a few surveys having been performed so far above 10 keV: the all-sky survey conducted in the 1980’s by the HEAO/A4 instrument in the 13-80 keV band (Levine et al. 1984) and more recently those of RXTE/PCA and Swift/BAT, in the 8-20 and 14-195 keV bands respectively (Revnivtsev et al. 2004, Markwardt et al. 2005). The latter, characterized by a positional uncertainty of  $\leq 3'$  and a flux detection limit of  $\sim 10^{-11}$  erg cm $^{-2}$  s $^{-1}$ , is the most accurate and sensitive survey to date at high energies. It covers the high latitude sky providing a sample of 44 active galactic nuclei (AGN), most of which are previously known from X-ray studies.

Despite being so rare, gamma-ray surveys are an efficient way to find AGN as they probe heavily obscured regions/objects, i.e. those that could be missed in optical, UV, and even X-ray surveys. Indeed, 64% of the non-blazar sources found by Swift/BAT have absorption in excess of  $10^{22}$  atoms cm $^{-2}$  and the overall column density distribution is bimodal. While none of the sources brighter than  $3 \times 10^{43}$  erg s $^{-1}$  shows high column densities, almost all weaker objects are absorbed. Quantifying the fraction of AGN missed by low energy surveys is necessary if we want to provide input parameters for synthesis models of the X-ray background and to understand the accretion history of the Universe.

A further step in this field is provided by the imager (IBIS) on board INTEGRAL, which, like BAT, is surveying a large fraction of the sky above 20 keV with similar sensitivity and positional accuracy. Analysis of the first year of INTEGRAL observations covering largely the galactic plane and centre has provided a first sample of 10 gamma-ray selected AGN (Bassani et al. 2004); more recently the second IBIS survey has listed 32 such objects (Bird et al. 2005). Detailed analysis of INTEGRAL observations also suggests that AGN are becoming a major constituent of the IBIS source population (Revnivtsev et al. 2005, Beckmann et al. 2005); at least 15% of the objects in the second IBIS catalogue are active galaxies. Here, we present a further step in our all-sky survey project, limiting the search to extragalactic objects. We have analysed  $\sim 11300$  INTEGRAL pointings and detected 62 AGN in the 20-100 keV energy range.

## 2. Data analysis

Data reported here belong to the Core Program and public Open Time observations and span from revolution 46 (February 2003) to revolution 309 (April 2005) inclusive; this represents a significant extension both in exposure time and area coverage with respect to the second IBIS catalogue (Bird et al. 2005) with more than 4000 extra pointings being

analysed. A detailed description of the data analysis and source extraction criteria can be found in the above reference, the only difference being the use of an updated version (4.2) of the standard OSA software.

To search for AGN we have used the 20-100 keV flux map, which provides a good combination between significance of detection and overall background level over the mosaic image: most AGN have power law spectra with  $\Gamma=1.9$  and a break around 100 keV (Malizia et al. 2003) and the energy band was selected to match these spectral characteristics. The threshold significance level used for the source extraction was  $5\sigma$ .

Staring data, which tend to be much noisier than dithering observations, as well as early exposures performed while the instrument set-up was still being finalized, were not included in the present mosaic; also sources detected only occasionally, e.g. in one or two revolutions only, are not considered in the present sample although they may be associated to flaring AGN such as blazars. Due to the different database used, our catalogue results may not include some sources already reported in the literature (e.g. Beckmann et al. 2005).

For each excess, the flux extracted from the 20-100 keV light curve was then used to estimate the source strength (up to 6% in flux can be lost in the mosaicing process) and independently confirm the image detection. Once a list of reliable excesses was produced, we proceeded to identify them by cross checking the IBIS error boxes (assumed to be  $3'$  as default) with the Simbad, NED (NASA/IPAC Extragalactic Database) and HEASARC (High Energy Astrophysics Science Archive Research Center) databases.

### 3. Soft Gamma-ray selected AGN

Of all the excesses found in this survey, we report in Table 1 only those which can be confidently associated with AGN. While some of the other detections may also be active galaxies, due to their location near the galactic plane it is difficult to discriminate them from galactic objects without further observations.

The 62 sources listed in the table are divided into two sections: (a) 32 objects already reported as confirmed or candidate active galaxies in the 2<sup>nd</sup> IBIS catalogue (all but one of the candidates have subsequently been confirmed as AGN through follow up optical spectroscopy (Masetti et al. 2005a,b)) and (b) 30 new objects, including four which were classified as unidentified in the 2<sup>nd</sup> IBIS survey but which we now consider to be AGN candidates. Between both sets there are 14 sources which have not yet any optical classification, but their extragalactic nature is strongly indicated either by follow up Chandra observations (IGR J07565-4129, IGR J12026-5349 and IGR J17204-3554), by their high latitude loca-

tion (IGR J13000+2529, IGR J13057+2036, IGR J16194-2810 and IGR J18429-3243) or by multiwaveband analysis using radio, infrared and X-ray archival data whereby their optical counterpart has been found to be associated with a galaxy (IGR J07597-3842, IGR J14552-5133, IGR J14492-5535, IGR J16558-5293, IGR J20187+4041, IGR J20286+2544 and IGR J21178+5139).

In the table, we list the relevant IBIS parameters (position, exposure and flux in mCrab) together with (where available) the optical classification and redshift obtained from NED archive or from more recent publications as detailed in the table. Between 20-100 keV, 1 mCrab corresponds, for a Crab like spectrum, to  $1.6 \times 10^{-11}$  erg cm $^{-2}$ s $^{-1}$  which is a value close to our detection limit. For objects with known distance, fluxes have been converted to gamma-ray luminosities assuming  $H_0=71$  Km sec $^{-1}$  Mpc $^{-1}$  and  $q_0=0$  (Spergel et al. 2003). Available column densities are also listed and have been obtained from X-ray data in the literature or in public databases. Unfortunately a significant fraction (about 30%) of our objects do not have archival X-ray spectra, so that an estimate of the column density must await X-ray follow up observations. The quoted column densities are intrinsic to the source, except for those cases where  $N_H$  is comparable to the galactic absorption, in which case the quoted values are upper limits.

About 40% of the objects listed in Table 1 are well known gamma-ray emitters and have been studied in the IBIS energy range by previous missions such as BeppoSAX, OSSE and RXTE; comparison of our data with past observations indicates overall agreement (within a factor of a few) on the flux (Soldi et al. 2005). The remaining objects are detected above 10 keV for the first time; many of these were not even known to be active nor to be X-ray sources before their INTEGRAL discovery (Sazonov et al. 2005). This is largely due to their location in the galactic plane which has prevented an in-depth study of these objects up to now.

A comparison of the IBIS catalogue with the Swift sample indicates that the intersection is very small (only 9 sources), due to BAT observing mostly the high galactic latitude sky while IBIS maps preferentially the galactic plane. It is likely that, together, these two surveys will provide a complete and deep sky coverage and thus the best yet sample of gamma-ray selected AGN for some time to come.

#### 4. Results and Conclusions

It must be remembered that the present survey is highly inhomogeneous in sky exposure and coverage, thus the present sample is far from being complete. Nevertheless a few inter-

esting considerations can be drawn by a simple statistical analysis. For objects with known distance, we plot in figure 1 the gamma-ray luminosity against redshift, to show the large range in these parameters sampled by the present survey. From this figure it is also evident that our sensitivity limit is around  $1.5 \times 10^{-11}$  erg cm $^{-2}$ s $^{-1}$  (straight line in the figure).

Within the overall sample, 42 objects are classified as Seyfert galaxies, 6 are blazars and 14 are still unclassified. Within the sample of Seyfert galaxies, 23 objects are of type 1-1.5 while 19 are of type 2 thus illustrating the power of gamma-ray surveys to find narrow line AGN. Excluding the blazars, the average redshift of our sample is  $0.021 \pm 0.017$  ( $1\sigma$ ) while the mean luminosity in Log is  $43.45 \pm 0.71$ . Assuming  $10^{22}$  atoms cm $^{-2}$  to be the dividing line between absorbed and unabsorbed sources, we find that absorption is present in  $65 \pm 17\%$  of the sample. This result is in line with the Swift findings (Markwardt et al. 2005) and above that found in X-ray surveys for bright objects (La Franca et al. 2005, Comastri 2004). It is also interesting to note that  $14 \pm 7\%$  of the total sample is due to Compton thick objects which is about three times the frequency found by Swift.

In figure 2 we show the column density of the sources as a function of IBIS luminosity. Although from this figure there is little evidence of any strong correlation, the few high luminosity objects in the survey all have low absorption. We can further investigate the relationship between  $N_H$  and Log(L) by forming the ratio between the fraction of absorbed sources above a given luminosity and that below this value. It can be seen from figure 3 that below  $\log(L) \sim 43.5$  the ratio is practically constant while above this luminosity it decreases sharply implying that at high IBIS luminosities there are very few absorbed sources. This is in agreement with that found by the Swift/BAT team and obtained from 2-10 keV studies (La Franca et al. 2005).

Within the sub-sample of 17 Seyfert 2s with known  $N_H$ , we find that all are absorbed and almost 30% are Compton thick; this is in line with previous estimates of the column density distribution of type 2 objects based on X-ray data (Risaliti et al. 1999, Bassani et al. 1999). Interestingly we also find that 33% of type 1 objects are absorbed.

More in depth studies of the present sample require optical classification of all objects and a detailed analysis of their broad band behaviour (particularly in the X-ray to gamma-ray band) in order to understand the role of absorption and the relation of extragalactic gamma-ray surveys to those in other wavebands. In the meantime this catalogue testifies to the power of INTEGRAL/IBIS to probe the extragalactic gamma-ray sky, discover new active galaxies and find absorbed objects.

## 5. Acknowledgements

This research has been supported by ASI under contract I/R/046/04. This research has made use of data obtained from NED (Jet Propulsion Laboratory, California Institute of Technology), SIMBAD (CDS, Strasbourg, France) and HEASARC (NASA’s Goddard Space Flight Center).

## REFERENCES

- Bassani, L., Dadina, M., Maiolino, R. et al. 1999, *Ap.J.S.*, 121, 473
- Bassani, L., Malizia, A., Stephen, J.B. et al. 2004, in *Proc. V INTEGRAL Workshop on the INTEGRAL Universe* (ESA SP-552, Noordwijk: ESA), 139
- Bassani, L., De Rosa, A., Bazzano, A. et al. 2005, *Ap.J.* 634, L21
- Beckmann, W., Soldi, S., Shrader, C.R., Gehrels, N. 2005, *Ap.J.* in press
- Bird, A., Barlow, A. J., Bassani, L., et al. 2005, *Ap.J.* 635,
- Collinge, M. J. & Brandt, W. N. 2000, *MNRAS*, 317, 35
- Comastri, A. 2004, in *Proc. Supermassive Black Holes in the Distant Universe*. Ed. Barger, A.J., *Astrophysics and Space Science Library* Volume 308, 245
- De Rosa, A., Piro, L., Tramacere, A. et al. 2005, *A&A*, 438, 121
- Donato, D., Sambruna, R. M. & Gliozzi, M. 2005, *A&A*, 433, 1163
- Guainazzi, M. 2002 *MNRAS*, 329, L13
- Levine, A., Lang, F., Lewin, W. et al. 1984, *Ap.J.S.*, 54, 581
- La Franca, Fiore, F., Comastri, A. et al. 2005, *Ap.J.* in press
- Lutz, D., Maiolino, R., Spoon, H. W. W. et al. 2004, *A&A*, 418, 465
- Malizia, A., Bassani, L., Stephen, J. B. et al. 2003, *Ap.J.* 589, L17
- Markwardt, C.B., Tueller, J., Skinner, G.K. et al. 2005, *Ap.J. Lett.*, 633, L77
- Masetti, N., Pretorius, M.L., Palazzi, E. et al. 2005a, *A&A* submitted
- Masetti, N., Mason E., Bassani, L. et al. 2005b, *A&A* in press

- Panessa, F. & Bassani, L. 2002, *A&A*, 394, 435
- Revnivtsev, M.G., Sazonov, S., Jahoda, K., Gilfanov, M. 2004, *A&A*, 418, 927
- Revnivtsev, M.G., Sazonov, S.Yu., Molkov, S.W. et al. 2005, *Astronomy Letters*, in press
- Risaliti, G.; Maiolino, R. and Salvati, M. 1999, *ApJ*, 522, 157
- Reynolds, C. S., Ward, M. J., Fabian, A. C. et al. 1997, *MNRAS*, 291, 403
- Sazonov, S.Yu., Revnivtsev, M.G. 2004 *A&A*, 423,469
- Sazonov, S.Yu., Revnivtsev, M.G., Lutovinov, A.A. et al 2004, *A&A*, 421, L21
- Sazonov, S. Yu., Churazov, E. Revnivtsev, M. et al. 2005, *A&A Lett.* in press
- Spergel, D.N., Verde, L., Peiris, H.V. et al. 2003, *Ap.J.S.*, 148, 175
- Soldi, S., Beckmann, V., Bassani, L. et al. 2005, *A&A* in press
- Torres, M.A.P., Garcia, M.R., McClintock, J.E. et al. 2004, *The Astronomer’s Telegram*, #264

Table 1. Table 1: Sample of Soft Gamma-ray selected AGN

Source#	RA	Dec	Exp(ks)	F <sup>†</sup>	Type*	z*	N <sub>H</sub> <sup>†</sup>	Log L <sup>†</sup>
AGN in the second IBIS catalogue								
QSOB0241+62	41.210	+62.481	159.9	4.3±0.4	S1	0.044	1.5±0.3 <sup>(1)</sup>	44.48
MCG+8-11-11	88.718	+46.447	33.8	5.4±0.8	S1.5	0.020	<0.02 <sup>(1)</sup>	43.90
IGR J07597-3842 <sup>a</sup>	119.948	-38.723	892.0	2.2±0.2	-	-	-	-
ESO 209-12	120.490	-49.757	1062.0	1.4±0.1	S1.5	0.040	-	43.92
Fairall 1146	129.649	-36.023	992.0	1.0±0.2	S1.5	0.031	-	43.54
MCG-05-23-016	146.895	-30.932	333.6	11.2±1.0	S2	0.008	1.6±0.2 <sup>(2)</sup>	43.45
IGR J10404-4625	160.105	-46.400	182.8	2.8±0.4	S2 <sup>A</sup>	0.024 <sup>A</sup>	>1 <sup>(3)</sup>	43.74
NGC4151	182.637	+39.400	56.2	35.4±0.5	S1.5	0.003	3±0.4 <sup>(1)</sup>	43.13
4C04.42	185.615	+4.253	208.0	2.2±0.3	B1	0.965	-	47.20
NGC4388	186.449	+12.652	62.3	16.5±0.7	S2	0.008	43±10 <sup>(1)</sup>	43.61
3C273	187.285	+2.036	270.0	8.3±0.3	B1	0.158	<0.03 <sup>(4)</sup>	45.92
NGC4507	188.904	-39.904	216.0	9.4±0.3	S2	0.012	29±2 <sup>(1)</sup>	43.66
LEDA 170194	189.807	-16.202	110.2	3.5±0.5	S2 <sup>B</sup>	0.037 <sup>B</sup>	1.9±0.3 <sup>(5)</sup>	44.23
NGC4593	189.917	-5.349	342.0	4.4±0.2	S1	0.009	<0.02 <sup>(1)</sup>	43.10
3C279	194.037	-5.777	318.0	1.8±0.2	B1	0.536	<0.02 <sup>(4)</sup>	46.46
NGC4945	196.358	-49.469	470.0	16.1±0.2	S2	0.002	400±80 <sup>(1)</sup>	42.29
CenA	201.363	-43.021	406.0	40.8±0.2	S2	0.002	23±13 <sup>(2)</sup>	42.67
4U1344-60	206.882	-60.619	732.0	4.2±0.2	S1 <sup>A</sup>	0.013 <sup>A</sup>	-	43.39
IC4329A	207.332	-30.314	236.0	12.5±0.3	S1.2	0.016	0.42±0.02 <sup>(1)</sup>	44.05
Circinus	213.282	-65.347	644.0	12.7±0.2	S2	0.001	360±70 <sup>(1)</sup>	41.97
IGR J16482-3036	252.050	-30.590	1644.0	2.0±0.1	S1 <sup>A</sup>	0.031 <sup>A</sup>	-	43.83
ESO138-G01 <sup>b</sup>	253.029	-59.218	572.0	1.4±0.2	S2	0.009	>150 <sup>(6)</sup>	42.60
NGC6300	259.234	-62.816	256.0	3.8±0.3	S2	0.004	29±2 <sup>(7)</sup>	42.25
GRS1734-292	264.369	-29.140	4040.0	5.1±0.1	S1	0.021	<0.5 <sup>(8)</sup>	43.92
2E1739.1-1210	265.466	-12.199	906.0	1.5±0.2	S1 <sup>C</sup>	0.037 <sup>C</sup>	-	43.87
IGRJ18027-1455	270.690	-14.917	1476.0	2.6±0.1	S1	0.035	-	44.06
PKS1830-211 <sup>c</sup>	278.413	-21.057	1950.0	3.1±0.1 <sup>e</sup>	B1	2.507	<0.26 <sup>(9)</sup>	48.53
ESO103-G35	279.695	-65.408	41.7	5.3±0.8	S2	0.013	15.1±0.5 <sup>(4)</sup>	43.51
2E1853.7+1534	283.984	+15.610	664.0	2.0±0.2	S1 <sup>B</sup>	0.084 <sup>B</sup>	-	44.73
NGC6814	295.666	-10.329	252.0	3.6±0.3	S1.5	0.005	<0.05 <sup>(4)</sup>	42.52
Cygnus A	299.869	+40.733	426.0	4.9±0.2	S2	0.056	38±8 <sup>(2)</sup>	44.75
IGRJ21247+5058	321.156	+50.970	438.0	6.1±0.2	S1	0.020	-	43.93
New AGN								
1ES0033+595	9.004	+59.833	776.0	0.9±0.2	B1	0.086	0.36±0.08 <sup>(10)</sup>	44.38
NGC788	30.264	-6.814	134.8	4.2±0.4	S2	0.014	21±0.5 <sup>(4)</sup>	43.43
NGC1068	40.704	-00.007	218.0	1.5±0.3	S2	0.004	>1000 <sup>(1)</sup>	41.88
NGC1275 <sup>d</sup>	49.878	+41.566	78.8	3.4±0.6	S2	0.018	1.5±0.7 <sup>(2)</sup>	43.57
3C111	64.611	+37.998	42.4	5.5±0.8	S1	0.049	<0.9 <sup>(4)</sup>	44.67
UGC3142	70.988	+28.960	71.7	3.9±0.7	S1	0.022	-	43.81
LEDA168563	73.054	+49.530	115.3	3.4±0.5	S1	0.029	-	44.00
MKN3	93.854	+71.044	468.0	4.8±0.2	S2	0.014	110±16 <sup>(1)</sup>	43.49
MKN6	103.040	+74.450	500.0	2.5±0.2	S1.5	0.019	10±0.6 <sup>(1)</sup>	43.48
IGR J07565-4139 <sup>e</sup>	119.080	-41.613	1078.0	1.0±0.1	-	-	1.1±0.2 <sup>(5)</sup>	-
QSO0836+710	130.320	+70.920	412.0	3.1±0.2	B1	2.172	<0.03 <sup>(4)</sup>	48.34
IGR J12026-5349 <sup>f</sup>	180.709	-53.820	334.0	2.5±0.3	-	0.028	2.2±0.3 <sup>(5)</sup>	43.83
IGR J12415-5750 <sup>g</sup>	190.368	-57.851	576.0	1.1±0.2	S2	0.024	-	43.35
IGR J13000+2529 <sup>h</sup>	195.022	+25.490	232.0	1.3±0.3	-	-	-	-



Table 1—Continued

IGR J13057+2036 <sup>i</sup>	196.422	+20.595	174.1	1.8±0.3	-	-	-	-
ESO323-G077	196.611	-40.445	336.0	1.6±0.2	S1.2	0.015	55±33 <sup>(11)</sup>	43.11
MCG-06-30-15	203.976	-34.297	324.0	3.1±0.3	S1.2	0.008	<0.02 <sup>(12)</sup>	42.81
ESO511-G030	214.849	-26.659	178.5	2.7±0.4	S1	0.022	<0.05 <sup>(11)</sup>	43.68
IGR J14492-5535 <sup>l</sup>	222.318	-55.587	814.0	1.2±0.2	-	-	-	-
IGR J14552-5133 <sup>m</sup>	223.811	-51.583	860.0	1.0±0.2	-	-	-	-
IGR J16119-6036 <sup>n</sup>	242.981	-60.597	600.0	1.5±0.2	S1	0.016	-	43.11
IC4518-A <sup>o</sup>	224.410	-43.129	770.0	1.7±0.2	S2	0.016	-	43.20
IGR J16194-2810 <sup>p</sup>	244.874	-28.110	526.0	1.7±0.2	-	-	-	-
NGC6221 <sup>b</sup>	253.029	-59.218	572.0	1.4±0.2	S2	0.005	1.1±0.1 <sup>(13)</sup>	42.07
IGR J16558-5203 <sup>q</sup>	254.014	-52.052	894.0	1.8±0.2	-	-	-	-
IGR J17204-3554 <sup>r</sup>	260.090	-35.909	3100.0	1.3±0.1	-	-	14±1 <sup>(14)</sup>	-
IGR J18249-3243 <sup>s</sup>	276.245	-32.715	2600.0	1.2±0.1	-	-	-	-
IGR J20187+4041 <sup>t</sup>	304.693	+40.697	576.0	1.4±0.2	-	-	-	-
IGR J20286+2544 <sup>u</sup>	307.156	+25.765	202.0	2.3±0.4	-	0.014	-	43.21
IGR J21178+5139 <sup>v</sup>	319.429	+51.671	408.0	1.6±0.3	-	-	-	-

Note. — † Fluxes (in units of mCrab with associated 90% error) and luminosities (in units of erg s<sup>-1</sup>) in the 20-100 keV band ; ‡ in units of 10<sup>22</sup> at.cm<sup>-2</sup>

∗: Type (S1-1.5= Seyfert 1-1.5; S2=Seyfert2; Bl=Blazar) and redshift according to NED or to: (A) Masetti et al. 2005a; (B) Masetti et al. 2005b; (C) Torres et al. 2004

# Notes to source detection: (a) IRAS 07579-3835; (b) analysis of various energy band mosaics indicates detection of both ESO138-G01 and NGC 6221, which are 11' apart; (c) lensed galaxy with magnification factor of ~10; (d) possibly contaminated by the Perseus cluster; (e) 2MASX J07561963-4137420, Sazonov et al. 2005; (f) WKK 0560, Sazonov et al. 2005; (g) WKK1263; (h) possibly MAPS-NGP O-379-0073388; (i) possibly NGP9 F379-1241685; (l) possibly 2MASX J14491283-5536194; (m) WKK4438 ; (n) WKK6092, but contamination by the nearby galaxy WKK 6103 is possible; (o) one of a pair of strongly interacting galaxies, so far the companion has not been classified as an active galaxy; (p) 1RXS J161933.6-280736; (q) possibly 1RXS J165605.6-520345=IRAS16520-5158; (r) NGC 6334B, Bassani et al. 2005; (s) possibly PKS1821-327; (t) 2MASX J20183871+4041003; (u) MCG+04-48-002 possibly interacting with NGC6921; (v) 2MASX J21174741+5138523.

References. — N<sub>H</sub> taken from: (1) Lutz et al. 2004; (2) Bassani et al. (1999); (3)Masetti et al. (2005a); (4)Tartarus database; (5) Sazonov et al. (2005); (6) Collinge & Brandt 2000; (7) Guainazzi 2002; (8) Sazonov et al. (2004); (9) De Rosa et al. (2005), ionized intrinsic absorption also possible; (10) Donato et al. 2005; (11) Sazonov & Revnivtsev (2004); (12) Reynolds et al. 1997; (13) Panessa & Bassani 2002; (14) Bassani et al. 2005.

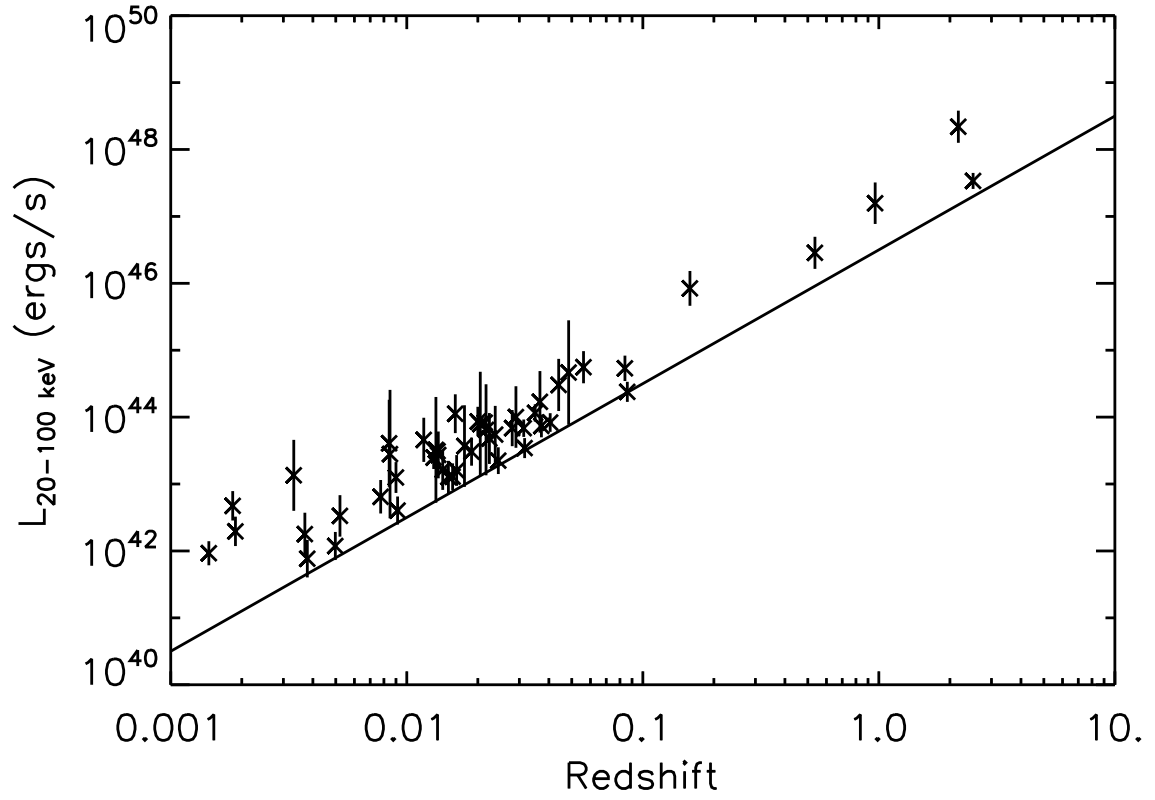


Fig. 1.— 20-100 keV luminosity versus redshift for optically classified AGN in the present survey; straight line corresponds to the IBIS survey limit

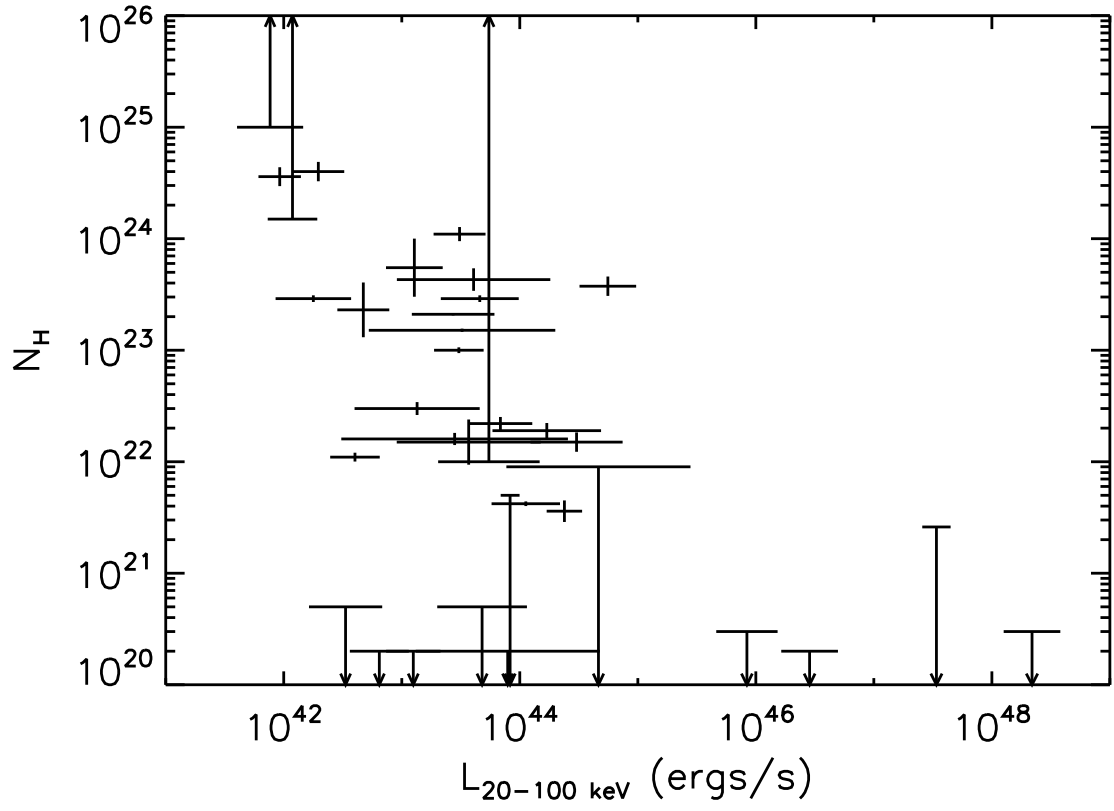


Fig. 2.— Column density versus 20-100 keV luminosity for AGN in the present survey with known intrinsic absorption

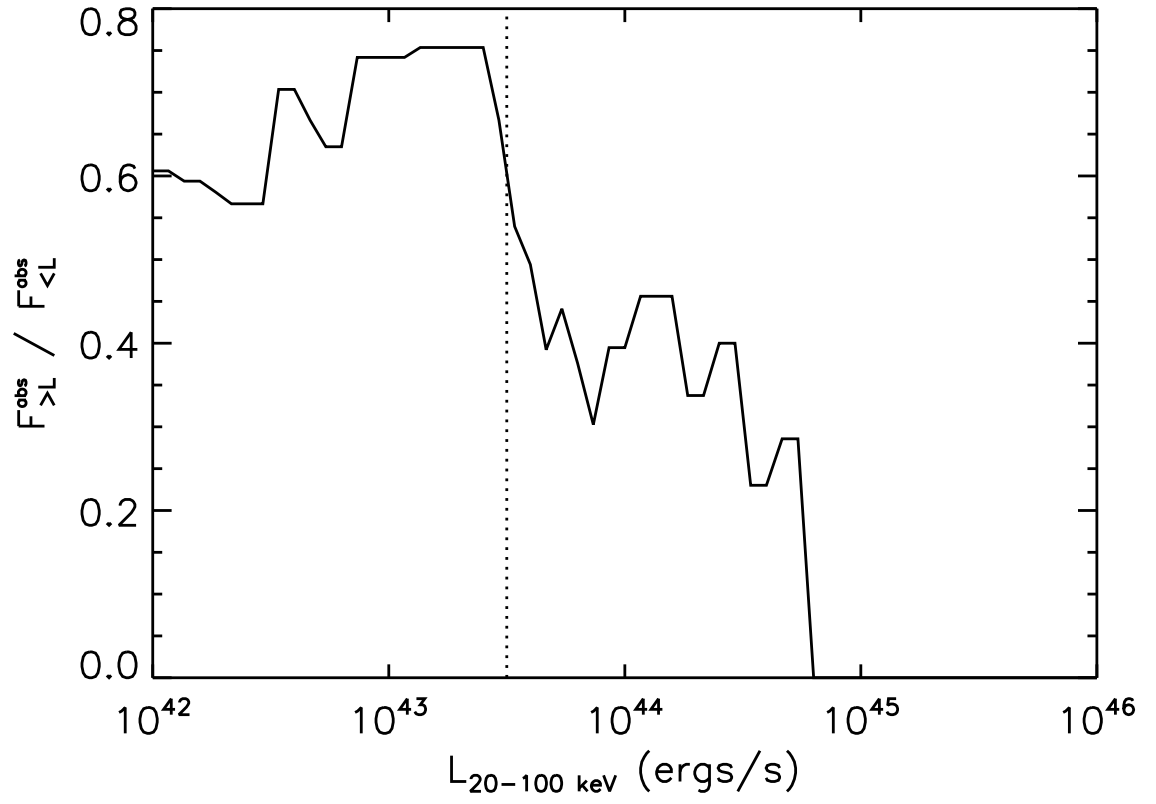


Fig. 3.— Ratio between the fraction of absorbed sources above a given luminosity and that below this value as a function of 20-100 keV luminosity